Design and fabrication of a passive integrated polarization splitter on the generic InP platform

K. Mehrabi[1], W. Yao[1], and J. J. G. M. van der Tol[1]

[1] Eindhoven University of Technology, Eindhoven Hendrik Casimir Institute (EHCI), 5612 AZ Eindhoven, Netherlands

An integrated fully passive polarization beam splitter on the generic InP platform is designed and fabricated. The birefringence of the waveguide is the only effect which is used for the beam splitting mechanism. The device is based on an asymmetric Mach–Zehnder interferometer with a curved waveguide in the upper arm and a straight waveguide in the lower arm to introduce π phase differences between the transverse electric (TE) and transverse magnetic (TM) modes. Measurement results at the wavelength of 1.55 µm indicated a splitting ratio of 11 dB and 20 dB for TE and TM input light, respectively. Since the designed device is based on the standard deep and shallow waveguides on the InGaAsP–InP platform it can be monolithically integrated with active and passive components, without any extra fabrication steps.

I. Introduction

In modern integrated photonics, polarization management is essential for enabling various applications, including optical communications, sensing, and computing [1]. Polarization splitters, which separate transverse electric (TE) and transverse magnetic (TM) modes, are critical components for polarization diversity and multiplexing. Traditional designs often rely on birefringence-induced phase shifts, but these designs can be highly sensitive to fabrication variations, requiring active tuning mechanisms, such as thermo-optic phase shifters, to correct for phase mismatches [2]. Although effective, such approaches increase complexity and reduce scalability. Fully passive polarization splitters and converters offer a more versatile and simpler alternative. Efforts to design passive polarization splitters have explored techniques like mode evolution and modal birefringence. While these methods have achieved low-loss and high-extinction ratio devices, they often result in lengthy devices that are unsuitable for compact integrated circuits. A passive polarization splitter (PS) that is robust against fabrication tolerances and compatible with large-scale photonic integration is therefore essential for scalable production. A compact PS on InP platforms, utilizing waveguide birefringence for phase control combined with a polarization converter is proposed [3]. However, such designs typically require additional lithography steps to create slanted waveguides for the polarization converter, complicating the fabrication process.

In this work, we present the design, fabrication, and characterization of a fully passive integrated polarization splitter implemented on the generic InP platform. Unlike active polarization splitters that depend on phase shifters to induce phase differences between TE and TM modes, our design eliminates the need for such components. This results in a cost-effective and simpler solution. However, this design has very small windows which has a high extinction ratio. The splitter consists of an asymmetric Mach–Zehnder interferometer (MZI) design, incorporating a shallow waveguide in the upper arm to minimize sensitivity to waveguide width deviations. A π phase shift between TE and TM modes is introduced through differential path lengths, ensuring robust performance without dependence on active tuning mechanisms. Measurement results demonstrate a splitting ratio of 11 dB for TE-polarized light and 20 dB for TM-polarized light at a wavelength of 1.55 µm. These results confirm the design's effectiveness. Additionally, the proposed fabrication process requires only three lithography steps, making it a practical and efficient solution for integration on the InP platform.

II. Design strategy

Figure 1 shows the schematic of the splitter. It operates as follows: the TE and TM modes first enter a 1×2 MMI, where they are split equally between two arms. The upper arm has a curved waveguide, while the lower arm has a straight waveguide, introducing phase differences between the TE and TM modes due to the length difference. The curved waveguide in the upper arm is designed for adding π phase shift difference between the TE and TM modes in the upper arm. To have a more compact device, we used deep waveguides for the entire circuit, except for the curved section, where we explored both deep and shallow waveguide designs to achieve a more fabrication-tolerant device. The cross-sections of the deep and shallow waveguides are shown in Fig. 2.Effective indices of TE and TM mode in the shallow and deep waveguides versus the waveguide widths are shown in Figure 3. As is indicated in this figure for the shallow core the modes effective index variation due to the widths deviation is lower than the deep waveguide and it can tolerate more deviation due to the fabrication errors. Table 1 shows the sensitivity of TE and TM modes for the deep and shallow waveguides at the widths of 1.5 µm and 2 µm, respectively. For TE modes using deep waveguide sensitivity increases with 22.22% as compared to the shallow waveguide. For TM modes deep waveguides are 20% more sensitive than shallow waveguides due to the widths variations. So, for the curved section, which induces a phase shift between the TE and TM modes, a shallow core was chosen to reduce sensitivity to width variations.. The length difference between two branches for π phase shift difference between the TE and TM polarization can be calculated as follows: $\Delta L = \frac{\lambda}{2(n_{TE}-n_{TM})}$
in which, λ is the operation wavelength, n_{TE}, and n_{TM} are the mode refractive indices for the TE and TM mode, respectively. So the curve length is equals to the ΔL plus the straight waveguide length (L_{WG}). For our layer stack the ΔL is achieved as 12 µm, while the waveguide length is 642 µm.

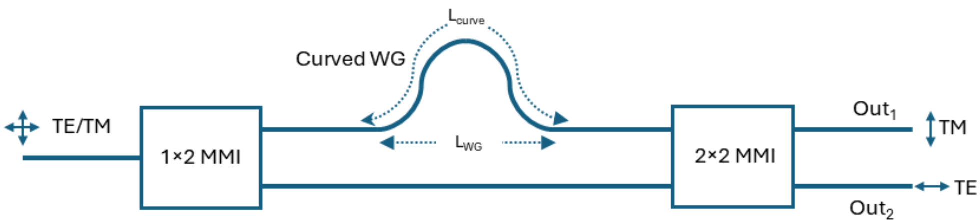

Fig. (1) Deep and Shallow waveguide cross section.

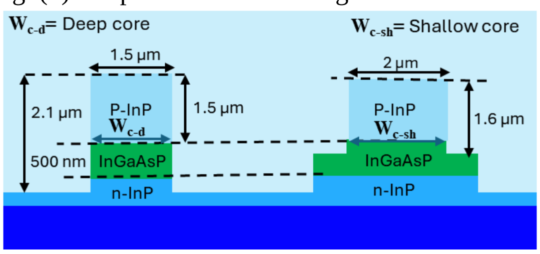

Fig. 2. Cross-section of passive deep and shallow waveguides in the generic InP layer stack.

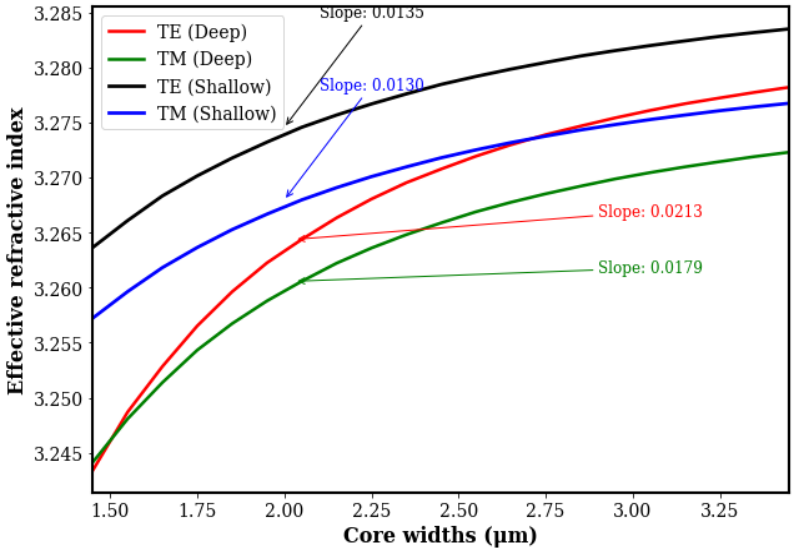

Fig. 3 Effective index of the deep and shallow waveguide as a function of widths.

Table 1. Variation in the refractive index for a 50 nm deviation in core widths of 2 μm for the shallow waveguide and 1.5 μm for the deep waveguide.

TE (Deep)	TM (Deep)	TE (Shallow)	TM (Shallow)
0.0011	0.0009	0.0007	0.0006

III. Fabrication

Since the device includes both deep and shallow waveguides, the process flow consists of three main lithography steps. The process begins with a passive layer stack grown on a semi-insulating InP wafer. The first step involves creating alignment markers using an ArF lithography scanner. In the second step, the waveguide pattern is defined, incorporating both deep and shallow waveguide regions, as shown in Fig. 4(a).. The third step involves protecting the shallow waveguides during the deep etching process (Fig. 4(b)). To minimize fabrication steps, the difference between the deep and shallow waveguides is first etched (Fig. 4(c)). Finally, after removing the resist, the sidewalls of all waveguides are etched, completing the process (Fig. 4(d)) to the required etch depths for the deep and shallow waveguides.

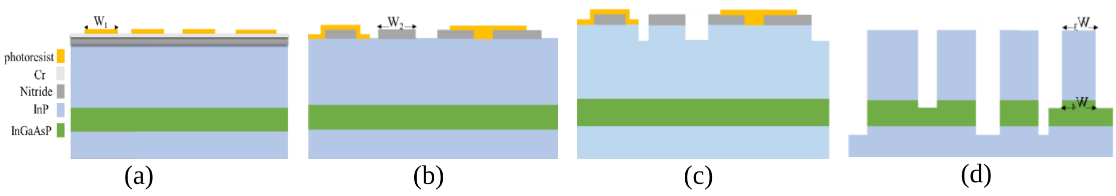

Fig. 4. Process flow of the PC fabrication on the generic InP platform.

IV. Characterization

The setup used for device characterization is shown in Fig. 5. The input polarization state is carefully defined using a polarization-maintaining fiber, followed by a fiber rotator to align the fast and slow axes of the fiber with the TE and TM modes at the chip facet. Another fiber rotator at the output couples the light into the fast and slow axis of the polarization-maintaining fiber connected to a polarization beam splitter. This setup measures the TE and TM components of the output signal. The characterization results for a ΔL of 12 µm are shown in Fig. 6. In this case, the waveguide length is 645 µm. The measured extinction ratios are 11 dB for TE-polarized input and 20 dB for TM-polarized input, validating the effectiveness of the polarization splitter.

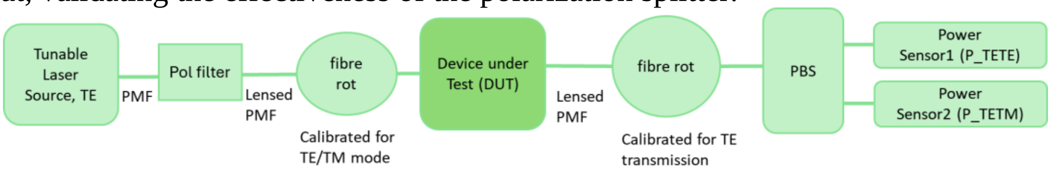

Fig. 5. Measurement setup for characterization of the polarization splitter.

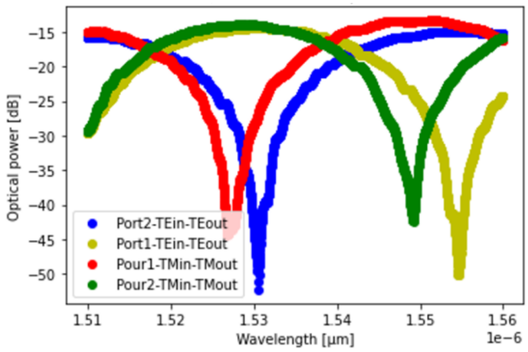

Fig. 6. Transmission of the TE and TM input signlat to the out_1 and out_2 for thr ΔL of 12 µm.

V. Conclusion

This paper introduces a passive polarization converter with a straightforward fabrication process. The sensitivity to fabrication deviations was analyzed through simulations and the shallow waveguide birefringence is used to apply phase shift difference between TE and TM mode. Experimental results demonstrate that the fabricated device achieves an extinction ratio of 11 dB for an input TE signal and 20 dB for an input TM signal at a wavelength of 1.55 µm. The performance can be further optimized by employing a wider waveguide and carefully selecting the device length, enabling both polarizations to achieve maximum extinction ratios at the same wavelength. However, the bandwidth of the device is small. These results highlight the device's potential for effective polarization splitter in the integrated photonic applications.

Acknowledgments

This work is funded by the H2020 ICT PICaboo project (Contract No. 101017114) under the photonics PPP.

References

[1] Vit, A. D., Rzayev, U., Danis, B. S., Amiri, A. N., Gorgulu, K., & Magden, E. S. (2024). Universal on-chip polarization handling with deep photonic networks. arXiv preprint arXiv:2411.16698.

[2] Dzibrou, D. O. (2014). Building blocks for control of polarization in photonic integrated circuits. [Phd Thesis 1 (Research TU/e / Graduation TU/e), Electrical Engineering]. Technische Universiteit Eindhoven.https://doi.org/10.6100/IR772730.

[3] Augustin, L. M., Hanfoug, R., Van der Tol, J. J. G. M., De Laat, W. J. M., & Smit, M. K. (2007). A compact integrated polarization splitter/converter in InGaAsP–InP. IEEE Photonics Technology Letters, 19(17), 1286-1288.